Variable-Friction Finger Surfaces to Enable Within-Hand Manipulation via Gripping and Sliding

Adam J. Spiers, *Member, IEEE,* Berk Calli, *Member, IEEE*,
and Aaron M. Dollar, *Senior Member, IEEE*

***Abstract*— The human hand is able to achieve an unparalleled diversity of manipulation actions. One contributor to this capability is the structure of the human finger pad, where soft internal tissue is surrounded by a layer of more rigid skin. This permits conforming of the finger pad around object contours for firm grasping, while also permitting low-friction sliding over object surfaces with light touch. These varying modes of manipulation contribute to the common ability for in-hand-manipulation, where an object (such as a car key) may re-positioned relative to the palm. In this work we present a simple mechanical analogy to the human finger pad, via a robotic finger with both high and low friction surfaces. The low friction surface is suspended on elastic elements and recesses into a cavity when a sufficient normal force is applied (~1.2-2.5 N depending on contact location), exposing the high-friction surface. We implement one 'variable friction' finger and one 'constant friction' finger on a 2-DOF gripper with a simple torque controller. With this setup, we demonstrate how within-hand rolling and sliding of an object may be achieved without the need for tactile sensing, high-dexterity, dynamic finger/object modelling or complex control methods. The addition of an actuator to the finger design allows controlled switching between variable-friction and constant friction modes, enabling precise object translation and re-orientation within a grasp, via simple motion sequences. The rolling and sliding behaviors are characterized with experimentally verified geometric models.**

I. Introduction

IT is easy to take for granted the wide range of manipulation actions that able-bodied people effortlessly make use of. Typical activities of daily living (ADLs), such as removing a key from a pocket and putting it into a lock involve the gripping, sliding and re-orientation of an object against the fingers and palm. A similar example comes from picking up a pen from a desk, then re-orientating it for writing. Such common within-hand-manipulation (WIHM) [1] tasks are considered difficult in robotics or prosthetics, where grippers have yet to closely imitate the sensory or manipulation capabilities of the human hand. Indeed, central to these given WIHM examples is the capability of the fingers to selectively grip and slide objects. These abilities are greatly aided by the mechanical structure of the human finger pad (Fig 1).

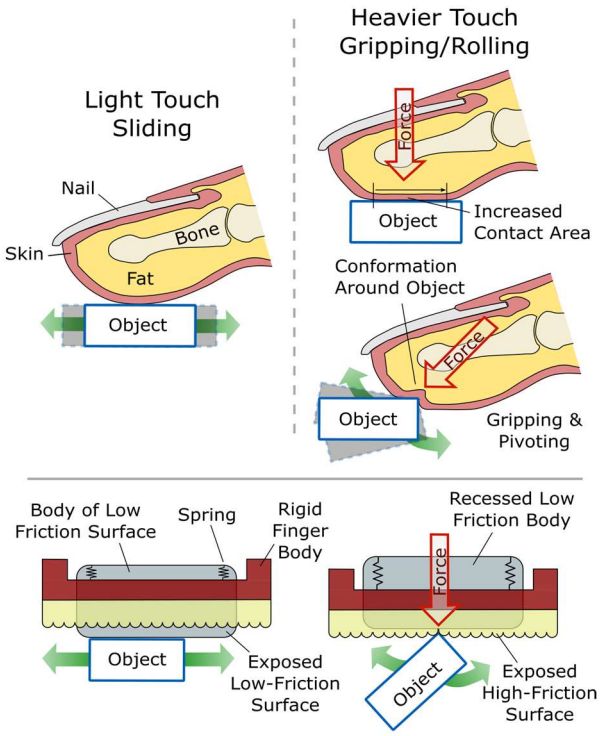


Figure 1. The human finger pad (top) can achieve sliding via light contact on the epidermal layer and gripping via compression of the glabrous fat by object features. The 'friction finger' (bottom) achieves a similar effect via a suspended low-friction surface, which recesses behind a high-friction surface when sufficient normal force is applied

The soft and pulpy tissue of the finger pad is able to conform and mold around objects, gripping them firmly when normal force is applied [2], [3]. Conversely the more rigid outer epidermal skin layer allows sliding over surfaces with light touch, supporting objects without securing them and enabling motions used for surface discrimination (i.e. stroking/rubbing) [4]–[6].

In robotics, many efforts have been made to replicate the functionality of the human hand, often via biological inspiration. On a material level, the benefits of soft 'skin' material on robot grippers has been shown [7], [8] in comparison to more rigid systems [3]. Such soft robotic skin

Manuscript received: February 24th 2018; Revised May 23rd 2018; Accepted 29th June 2018.

This paper was recommended for publication by Editor Han Ding upon evaluation of the Associate Editor and Reviewers' comments. This work was supported in part by the National Science Foundation grant IIS-1317976.

When this work was completed all authors were with the Department of Mechanical Engineering and Materials Science, Yale University, New Haven, CT 06511 USA. E-mail: a.spiers@is.mpg.de, berk.calli@yale.edu, aaron.dollar@yale.edu

Digital Object Identifier (DOI): see top of this page.

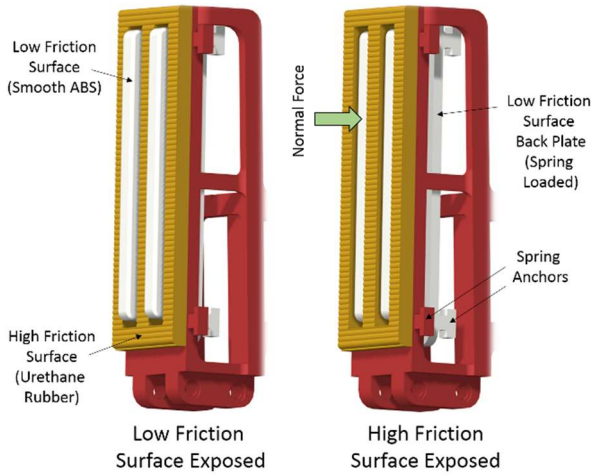


Figure 2. Structure of the passive Variable Friction (VF) finger. Elastic elements suspend the low friction surface through cavities in the high friction surface.

is typically a homogenous rubber that provides a compromise between compliance and strength [4], but does not achieve the same dynamic properties as the layered skin and fat of glabrous (smooth & hairless) finger tissue [4], [7].

In this work, we propose a new design of a robotic finger that uses a simple passive mechanism to enable a significant change in the coefficient of friction (see Section III.A) and morphology of the contacting surface to either slide over objects or grip them, as in the human finger [9]. When the fingers are implemented in a simple gripper, objects may pivoted (rotated) and translated within a grasp (Fig. 1 bottom).

Though our functional object-manipulation goal is biologically inspired, our approach does not directly replicate the form of the human finger (unlike [4]). Instead, we rely on a simple mechanism that uses elastic elements to suspend a low friction, rigid finger surface (smooth 3D-printed ABS) through cavities in a high-friction deformable surface ('Vytaflex 30' Urethane Rubber). When these 'Variable Friction' (VF) fingers exert low (<1.2 N) normal forces on objects, the low friction surface remains exposed, allowing the finger to behave as if it was made of smooth plastic. Once the normal force exceeds that of the elastic elements, the low-friction element is pushed into the cavity of the high-friction element, exposing the soft and textured high-friction surface.

In this paper we present two different variations of this general concept. One uses a purely passive VF finger pad, where the low friction element (colored white in Fig. 2) is simply supported by a passive spring such that a sufficiently large contact force can push it away. In the second implementation the low friction element continues to be supported by the spring, but may also be actively retracted via a small servo, exposing the high-friction surface. Both of these are implemented in simplistic 2DOF robotic grippers: the first with one passive VF and one 'constant friction' (CF) finger (in which no low friction element is present) (Fig. 3), and the second with two actively variable friction fingers (Fig. 4).

Using these grippers, we demonstrate how varying friction properties can enable planar sliding and rolling

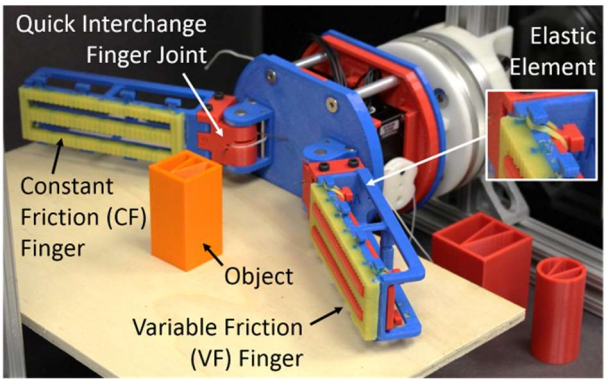


Figure 3. Experimental setup with passive (non-actuated) VF and CF fingers mounted on the 2DOF hand. The CF finger is the same as the VF finger but with no low-friction insert.

WIHM actions to be achieved in low dexterity systems without complex controllers, dynamic models or tactile sensing. Indeed, only open-loop position and torque control is required on the two drive actuators to achieve these dexterous motions.

In comparison to the passive system, we demonstrate that by selectively alternating friction between the fingers, we can greatly expand manipulation capabilities, allowing objects to be rotated and positioned to arbitrary locations throughout the workspace. We believe that the results of this simple, initial implementation is indicative of richer WIHM (such as the motivating ADL examples given at the start of the paper) that may be achievable when the VF finger concept is applied to more complex robotic or prosthetic hands.

II. Related Work

A. Biological Inspiration / Finger Properties

Though many aspects are involved in object manipulation, friction plays a key role, with the frictional properties of biological skin having been investigated by a variety of disciplines [10]. The mechanics of skin contact are

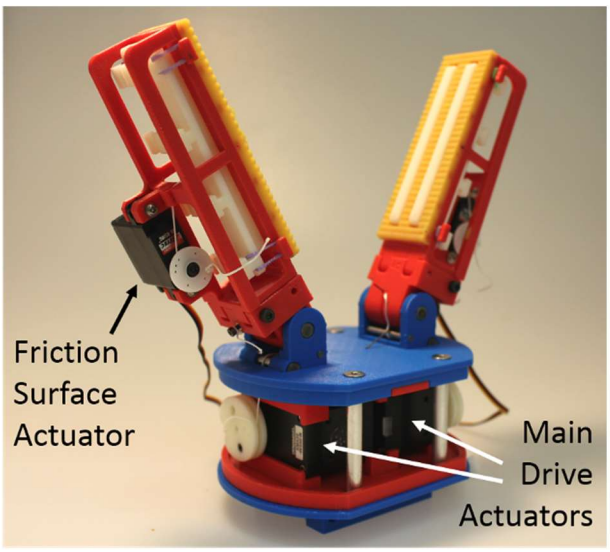


Figure 4. The 2DOF gripper with two 'Active VF fingers', which use hobby servos to retract the spring loaded low-friction finger surface, changing the VF fingers to Constant Friction (CF) fingers.

complex and governed by factors such as ridges and sweat produced by the finger pads [5]. The deformability of the finger pad also leads to increasing contact area with normal force application. In [11] it was claimed that fingertip frictional force is dependent on this contact area and so has a non-linear relationship to normal force. This was partially disputed in [10], [12] who state that this only holds true before 1N of normal force deforms the finger into its limit of compressibility. After this point, it behaves as a rigid body, with friction force linearly proportional to normal force.

Mechanically replicating the desirable properties of human finger pads has been a goal in robotics for some time [7]. The layered structure of the thin, epidermis surrounding the soft core gives the glabrous skin the strength and high compliance to grip, lift, explore and manipulate objects while also permitting light touch and the transmission of fine tactile information to nerve endings [6].

Though we have been unable to find many other examples of manipulation surfaces that can vary their coefficient of friction for manipulation, associated work follows. In [13] cylindrical rubber fingers with alternating hollow/rigid internal sections were proposed as a way of achieving various manipulation modes, particularly pivoting. However, surface friction did not vary and finger pad compression behavior depended on contact location. An elastic mounted pivot-point modification to a parallel jaw gripper in [14] enabled cylindrical objects to be passively re-orientated from horizontal to vertical orientation via gravity, then firmly grasped. However, no further WIHM was possible beyond this. Similar gravity-based pivoting between passive rotating fingertips is shown in [15], which also considered sliding or dragging objects across a 'ground' surface. In micro/nano-scale manipulation, adhesion between manipulators and objects is a studied phenomenon [16], though this behavior does not translate to the macro scale. The authors of [17] proposed using a matrix of capacitive MEMS actuators to change the shape of robot fingertip skin for different tasks, which would also change frictional properties.

Variable friction has been considered in robot locomotion. A soft robot inchworm in [18] features a foot with adjacent surfaces that have different frictional properties. The contact of each frictional surface with the ground depends on 'leg' pose. Furthermore, electrostatic adhesion selectively applied traction to the feet of an undulating soft-robot in [19].

Haptic interfaces have been developed that change the amplitude of vibrating plates to vary effective friction on a human finger [20]. This effect has added tactile sensations to touch screens, but has not been used for manipulation.

Finally, the 'Velvet Fingers' implement active conveyor belt finger surfaces to impart thrust on objects for WIHM [21]. Though that paper also discuss the potential of variable adhesion surfaces to achieve WIHM, that technique was not implemented in a physical prototype. Note that the mechanical complexity of the Velvet Fingers is prohibitive to replication ([21], Figs. 13-16) while the VF fingers are designed for cheap and easy fabrication, in the style of the Yale OpenHand [22].

B. Within Hand Manipulation

Within-hand-manipulation (WIHM) is defined in [1] as producing the motion of an object within the hand (i.e. in a prehensile grasp) via parts of the hand moving with respect to a frame fixed at the base of a hand. Such manipulation is classified as 'dexterous manipulation' via resulting rotational or translational object motions [1]. WIHM is beneficial to humans and robots by enabling object repositioning without either gross arm motion or bi-lateral (two handed) interactions. This enables tasks to be performed faster, with less energy expenditure and in confined spaces. For example, permitting WIHM in industrial pick-and-place scenarios would reduce robot cell volume requirements for tasks involving object re-orientation. A longer-term goal of WIHM in upper-limb prosthetic grippers (which are not necessarily anthropomorphic) could lead to amputee users achieving the ADL tasks described in Section 1.

Past efforts at robotic WIHM have typically resulted in high-DOF anthropomorphic mechanical systems [23], [24] and/or model-dependent control approaches with in-depth pre-planning [25]–[27]. Chong et al. [25] formulated rolling and sliding as a non-linear optimization problem in a quasi-static case while Shi et al. [27] solved forward and inverse finger and objects dynamics in a highly instrumented environment in order to achieve within-hand object sliding.

Various groups have attempted to understand the mechanics of object sliding/slip [28], [29] or rolling [3] for controlled reproduction in robotic WIHM. The resultant extensive modelling has incorporated frictional effects for dynamic and quasi-static cases in [30], [31] and frictional limit surfaces [8], [32], [33] for various contact assumptions.

A non-model based approach to WIHM is apparent in [9], where a gripper was designed based on kinematic observations of human hand motion during WIHM precision translation and re-orientation tasks. Neither finger/object dynamic models nor trajectory planning were implemented.

III. Materials

A. Mechanical Components

Construction of the VF fingers is based upon the fabrication process of the open-source Yale OpenHand [22]. The finger body is 3D printed from ABS using a Stratasys Fortus 250mc with a thin walled cavity that forms a mold for the compliant, high-friction finger pad. A removable insert forms the cavities for the low-friction insert (Fig. 2) while the mold is filled with a urethane elastomer (Vytaflex 30, manufactured by Smooth-On, Inc). After curing, a saw is used to remove the thin walls of the cavity. The removable molding insert is then replaced with the low-friction element, which is also 3D printed in ABS. Constant Friction (CF) fingers are simply VF fingers without the low-friction element. These fingers always make use of the high-friction, molded surface.

The high-friction finger pads measure 30×95mm. The low friction inserts consist of two rectangular sections, joined by a common base. Each rectangular section is 5.5mm wide and 80mm long with a separation of 7.5mm. When no normal force is applied, these protrude 1.25mm beyond the ridges of the high-friction surface. The ridges on high-friction finger

pad have a depth of 0.6mm and a spacing of 3mm. The body of the urethane finger pad is 4.6mm thick, but contains a number of ABS anchors from the finger body, in order to keep it attached.

The coefficient of static friction for the low and high friction finger surfaces were determined by placing an active finger in contact with a sheet of aluminum and a flat ABS surface, also printed by the Stratasys Fortus printer (the manipulation objects are also fabricated in this way). When in contact with aluminum, the static friction coefficients are 0.315 and 0.692 for the low and high-friction surfaces. When in contact with ABS, the low and high static friction coefficients are 0.125 and 0.688. Modifying the friction surface therefore changes the coefficient by a factor of 2.2 (against aluminum) and 5.5 (against ABS).

Four elastic dental bands (1/4" 'heavy' variety, manufactured by Essix) act as springs to attach and suspend the corners of the low-friction element from the main body. This arrangement allows the low-friction surface to recess into the high-friction cavities out-of-plane. The lack of guide structures means that distal/proximal object contacts exert forces primarily on the nearest two elastic elements, while central contacts will engage all four elastic elements. As such, the stiffness of the suspended low-friction element changes over its length. The stiffness has been measured at 942N/m near the fingertip (distally), 1962 N/m at the finger center and 1255 N/m near the base (proximally). As such, respective normal forces of 1.18 N, 2.45 N and 1.57 N are required to overcome the elastic elements and expose the high-friction surface. These proximal and distal values are similar to the 1 N limit of compressibility of the human finger [10], [12]. Note that we have not had to represent this variation in stiffness in our control algorithms, as we simply ensure that normal force application for high-friction manipulations exceed 2.45 N.

For the actuated versions of the VF fingers, HiTec HS-85MG servo motors were mounted on the back of the fingers (Fig. 4). Tendons are attached between the servo horns and low friction element back plate, so that rotation of the servo pulls the low-friction element behind the high-friction element (this requires 2.45 N on the tendon). This converts the VF finger to a CF finger. Note that when the low-friction surface is not retracted by the servo, it continues to acts as a passive system, dependent on the elastic elements (i.e. the servo does not 'push' the back-plate into a low-friction mode).

The 2DOF gripper (Fig. 3 and 4) comprises of two VF/CF fingers are mounted on T42 OpenHand base [22] which has been updated to accommodate Dynamixel Model-X actuators. The gripper features one rotational DOF at the base of each finger. This joint incorporates a quick-disconnect interface that permits fingers to be easily substituted for one another without tendon re-tying and joint disassembly. As with other models of OpenHand [22], [34], the fingers are tendon driven in closure with a torsion spring return mechanism. The VF hand is compatible with other OpenHand components to allow easy mounting on a variety of robot platforms. The design files will be made available on www.eng.yale.edu/grablab/openhand

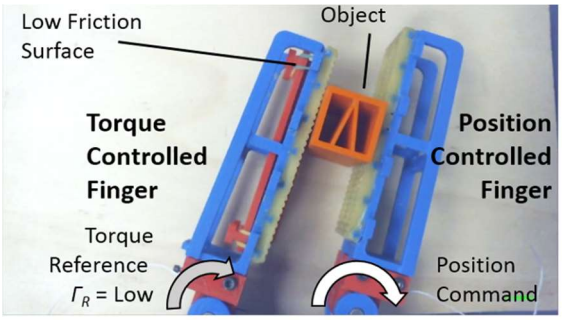


Figure 5. The finger pushing the object (left in the above scenario) is always torque controlled. The other finger is position controlled and leads the motion. By changing the torque reference, the high and low friction surfaces may be engaged for different manipulation behaviours.

B. *Control Approach*

Our simple control approach makes use of the integrated position and torque control modes of the Dynamixel Model-X actuators and switches their role between fingers to maintain object contact during manipulation, while also having the capability to adjust normal force application. Software to control the VF hand was implemented in ROS.

After establishing an initial grasp on an object, motion of the fingers begins. Regardless of motion direction, torque control is applied to whichever finger is currently pushing (moving towards) the object. Position control is set to the other finger (Fig. 5). The torque control functions by setting a target torque reference (Γ_R) to either a low (0.25 Nm) or high (1 Nm) value. As the position controlled finger moves, the 'pushing' finger attempts to maintain the torque reference. This causes the VF finger to sustain contact with the object during motion, while also attempting to apply a constant normal force. By adjusting the torque reference, it is possible to modify the normal force applied onto the object by the current pushing finger. The magnitude of this normal force determines the compression of the suspended low-friction surface, as illustrated in Fig. 1 and 2. If a low-torque reference is provided, the low-friction surface of the VF finger will remain exposed during manipulation, enabling sliding of an object (Fig. 1 bottom left). If a high-torque reference is provided, the high resulting normal force will push the low-friction surface behind the high-friction surface, causing the VF finger to grip and roll the object (Fig. 1 bottom right). In short, manipulating an object between the fingers with a low-torque reference enables object sliding (translation), while manipulating with a high-torque reference enables pivoting. This will be demonstrated in the next section.

A nonlinear relationship was observed between actuator torque and the position (q_{VF}) of the (unloaded) VF finger (due to the torsional return spring, cable routing around multiple elements and inter-part friction). To counter this, a feedforward term is applied to the torque reference to improve consistency of normal force application over the finger workspace. This term is derived automatically by a calibration routine in which actuator position is sampled as torque is linearly increased. A quadratic curve of degree three is fit to the sampled data to model the position/torque relation.

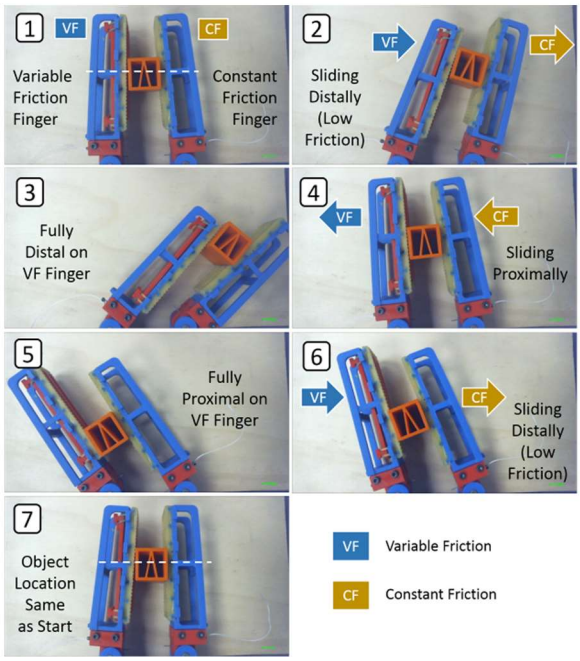


Figure 6. Sliding of a square object along the Variable Friction (VF - left) finger by using a low torque-reference to maintain exposure of the low friction surface. Note that the object is forced to remain at the same location on the Constant Friction (CF - right) finger throughout.

$$\Gamma_R = \Gamma_{FF}(q_{VF}) + \Gamma_D, \quad (1)$$

$$\Gamma_{FF} = a(q_{VF})^3 + b(q_{VF})^2 + c(q_{VF}) + d \quad (2)$$

Where Γ_{FF} is the feedforward term, which is a function of the current angle of the VF signified as q_{VF}. Γ_D is the desired torque while Γ_R is the resultant torque after the feedforward term Γ_{FF} has compensated for the torque / position non-linearity. The terms *a, b, c,* and *d* are the coefficients of the quadratic function estimated via the calibration routine.

Note that currently the control techniques are run in a scripted and open-loop fashion, to demonstrate the principle and manipulation capability of the VF fingers. It is clear however that automated and precise pose control would be a relatively straightforward future addition to the system.

IV. Implementation

In this section we demonstrate the manipulation capability of the VF fingers. Most of the examples make use of a square profile ABS object (measuring 25.4×25.4×50.8 mm), though manipulation with other objects will also demonstrated.

A. Passive Finger Object Translation

Fig. 6 illustrates the object sliding (translation). Beginning with a grasp of the object in the center of the workspace (step 1), a low torque reference is applied and held on the VF finger. The CF finger is then rotated clockwise (step 2, 6) and anticlockwise (step 4). The low torque-reference causes the VF finger to follow these motions by maintaining contact with the object, while also keeping the low-friction surface exposed, due to low normal force (<1.2N). As the CF finger is rotated, the object slides along the surface of the VF finger, reaching the distal (step 3) and proximal (step 5) regions. While sliding occurs on the VF finger, the object keeps the same location on the high-friction CF finger.

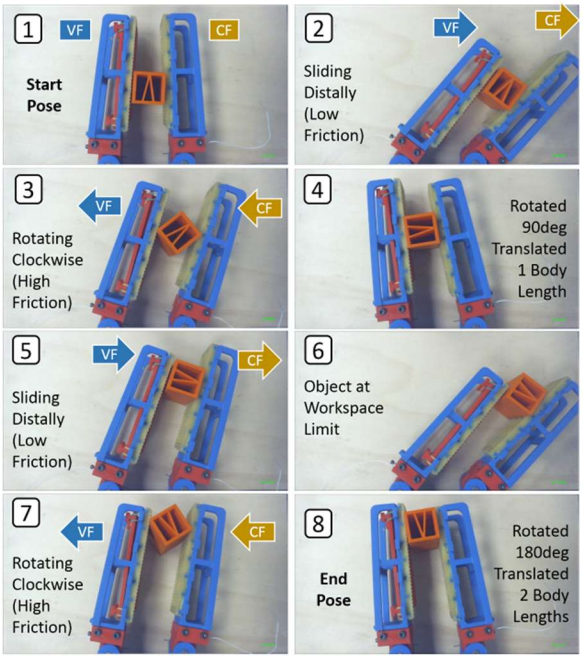


Figure 7. By applying a high torque-reference at steps 3 and 7, the VF finger engages the high-friction surface, enabling object pivoting/rotation. A low torque-reference enables object sliding on the low-friction surface in steps 2 and 5. Note that rotation cannot be achieved without object translation in this passive configuration.

Though this method demonstrates effective bi-directional sliding along the VF finger, the inability of the object to slide on the CF finger means that the object is unable to translate in the overall grasp (e.g. relative to the base of both fingers).

B. Passive Finger Object Rotation

In Fig. 7 the object is first translated distally via sliding on the low-friction surface (steps 1-2) by moving the position controlled CF finger clockwise while applying a low reference torque to the VF finger. The object is then rotated clockwise by moving the fingers anti-clockwise (step 3-4). This change in direction changes the role of the VF finger to position controlled and the CF finger to torque controlled. A high-reference torque is applied to this motion. The resulting increase in normal force within the grasp exposes the high-friction VF finger surface. This engages the object in a gripping and pivoting motion as the fingers move. This sliding and rolling process is repeated again (steps 5-8), demonstrating that each rotation is also associated with a distal translation of the block by 1 body length. Following step 8 it is only possible to change the position of the object

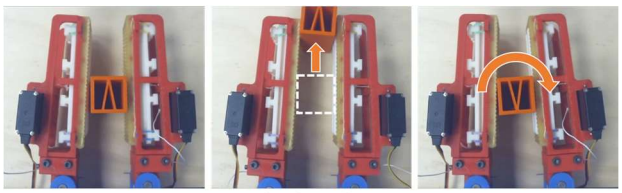


Figure 8. Active fingers enable enhanced control of object pose, negating the translation limits or rotation/translation coupling demonstrated with the passive finger (Fig. 6 and 7).

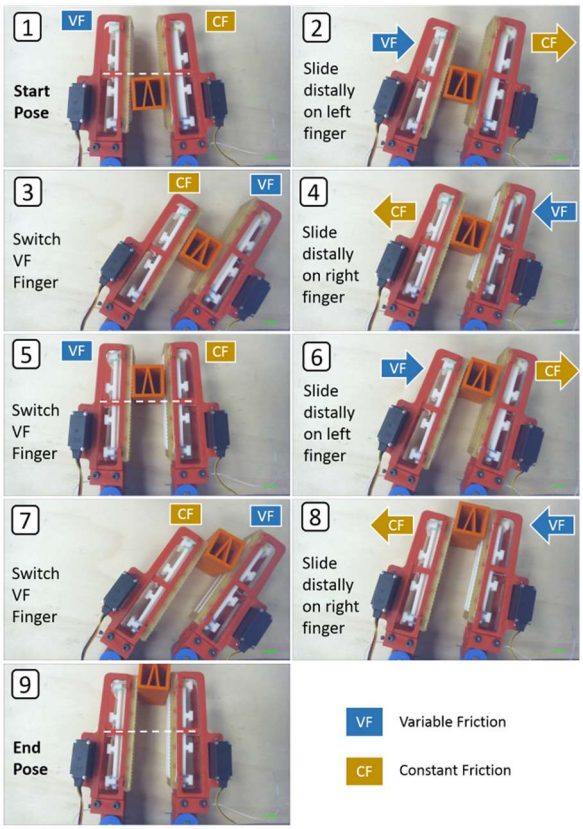


Figure 9. Translating an object distally from the middle of the grasp by switching the CF and VF finger roles (and therefore low-friction and high-friction surfaces) between left and right digits on steps (3, 5 and 7). A low-reference torque was maintained throughout.

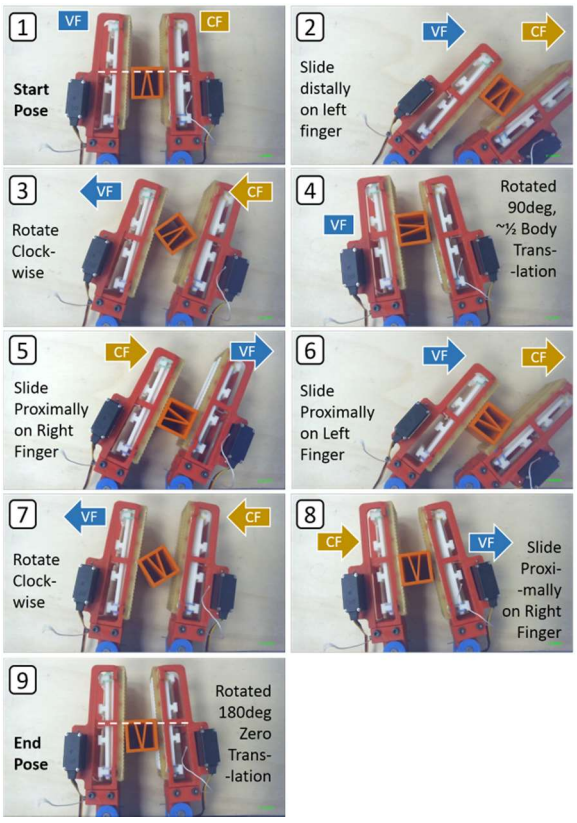


Figure 10. The actuated fingers make it possible to change the object's orientation, while also controlling its position via controlled sliding on both fingers. Here, the object starts and ends with its top face aligned with the center of the fingers, despite rotating 180degrees.

on the CF finger by returning to step 6 or ejecting the object from the grasp. As in the previous example, this is because translation is not possible on the constant high friction surface of the (right) CF finger.

C. *Active Finger Motivation*

The passive finger examples have highlighted the capability of the VF/CF finger combination for rolling and sliding with simple control. These examples have also highlighted the limitations of the CF finger, due to a lack of sliding capability. Unfortunately this cannot be remedied by using two passive VF fingers, as the object must be anchored on one high-friction surface to permit sliding on the low-friction surface. Our solution to this issue has been to create fingers that can change their role from VF to CF, via a small additional actuator (described in Section III.A). This development continues to use the same control approach as the passive fingers, with torque/position control assigned based on movement direction, yet object translation and rotation (i.e. 'pose') may now be independently manipulated (Fig. 8).

D. *Active Finger Object Translation*

Fig. 9 illustrates the distal translation of an object from the center of a grasp to the fingertips of both fingers. This motion is commonly used in human manipulation for such tasks as transferring a key from a power to pinch grasp. Here, the distal translation technique functions by sequentially:

1. Assigning the right finger to CF and left to VF (step 1)
2. Rotating the fingers clockwise, causing the object to slide distally up the VF finger (step 2)
3. Switching the finger roles, so the left finger is CF and right is VF (step 3)
4. Rotating finger anticlockwise, causing the object to slide distally up the VF finger (step 4)
5. The sequence is repeated in steps 5-9 (Fig. 9).

This technique may also be reversed to move an object proximally. As object translation (on both fingers) is not coupled to object rotation (as in Fig. 6), the object may be translated by any distance within the grasp. This is achieved by determining the degree of finger rotation in steps 2, 4, etc.

E. *Active Finger Object Rotation*

Fig. 10 illustrates how an object may be rotated to a target pose without a coupled final translation. Object rotations with the 2DOF hand inevitably involve translation, due to the method of pivoting on a corner. However, the fine translational control discussed in the previous example (Fig. 9) allows the gripper to slide the object back to its starting position.

F. *Manipulation with Other Objects*

Fig. 11 illustrates manipulation with a larger (38.1mm) square object and a 25.4 mm cylinder. In past approaches [25]–[27], object models are used to plan rolling and sliding manipulation. As previously mentioned, our approach currently uses simple open loop control with scripted motions to achieve target poses. To test manipulation with these new

objects the amount of finger rotation was modified (to be greater for the cube and smaller for the cylinder) but the torque references remained as before. The larger square object rotates and translates in a similar fashion to the original square object, though the fingers must travel further across their workspace to facilitate a 90 deg rotation (steps 2-4), in comparison to the original object (Fig. 10). Note that the control approach in Fig. 11 does not aim to achieve the same start position of the cube. Predictably, the cylinder object rotates (by ~90 deg) during the sliding action (step 2), in addition to translating. The cylinder is also successfully rotated clockwise during the rotation action (step 3). The end pose of the object therefore resembles the start pose. This is to be expected, as sliding round objects is difficult even with the human hand.

G. Discussion on the Gripper Workspace

Though the proposed gripper design is not underactuated (in total it has two finger joints driven by two actuators), the hand-object system is underactuated, as we are aiming to control both the object's x and y-position together with its orientation. Nevertheless, our system can achieve arbitrary poses of the object via planning non-holonomic motions by switching between sliding and sticking modes. In other words, variable friction surfaces allow us to change the motion manifold of the object, which provides a within-hand manipulation workspace beyond the majority of the gripper designs in literature.

V. Geometric Model

To better understand the behavior of the VF fingers, we have determined geometric models of the characteristic manipulations (Fig. 12). In the sliding case, adhesion of the object to the CF finger and contact with the VF finger allows the system to be modelled by a slider crank mechanism. In this representation, w_P is the palm width (distance between finger joints), w_O is the object width, d_{CF} is the position of the object's bottom corner on the CF finger (measured from the finger joint) and d_{VF} is the position of the object's bottom corner on the VF finger, which changes during manipulation. A_{BC} and θ_{CF2} connect the CF finger joint and the bottom corner of the object. The distance from the center line of the fingers to the pad is represented by F_W. Using the following model, we can determine the change in object position d_{VF}, and VF finger position θ_{VF} for a given change in the CF finger position, θ_{CF}.

$$\theta_{CF2} = \pi - \left(\theta_{CF} + atan\left(\frac{w_O + F_w}{d_{CF}}\right)\right) \quad (3)$$

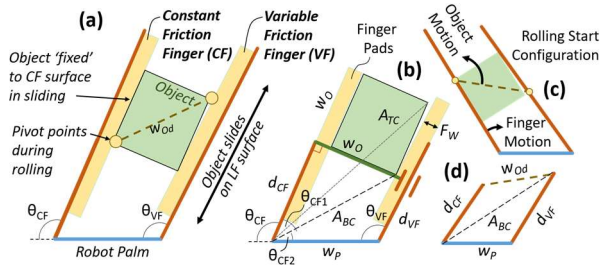


Figure 11. Sliding is modeled by a slider-crank *(a,b)* while rolling is modelled as a 4 bar mechanism *(c)*, with the final pose as *(d)*.

$$d_{VF} = \sqrt{F_W^2 + {A_{BC}}^2 + {w_p}^2 - 2A_{BC}Aw_p\cos(\theta_{CF2})} \quad (4)$$

$$\theta_{VF} = \text{acos}\left(\frac{{d_{VF}}^2 + {w_P}^2 - {A_{BC}}^2}{2d_{VF}w_p}\right) \quad (5)$$

Depending on workspace location, the VF finger will make contact at either the top or bottom object corner. This is determined by performing the same calculations with A_{BC} (bottom contact) and A_{TC} (top contact), as shown in Fig 12.a. The greatest resulting magnitude of θ_{VF} identifies the contact.

For rolling behavior of square objects, the system may be treated as four bar linkage/irregular quadrangle, formed via the sides *wp, d_{CF}, w_{Od}* and d_{VF} (Fig. 12.d). Note that though both fingers are in high-friction mode during rolling, we use the same CF/VF nomenclature as the sliding example for simplicity, though the CF finger will now be referred to as the 'pushing finger' due to its role in the rolling manipulation. In rolling, d_{CF} and θ_{CF} are known initial conditions of the systems, with equations (3-5) allowing the calculation of d_{VF}. We may then calculate the final pushing finger angle (θ_{CFE}) necessary for a 90deg object rotation::

$$\theta_{CFA} = \text{acos}\left(\frac{(d_{CF} + w_O)^2 - 2w_O^2 + {A_{BC}}^2}{2A_{BC}(d_{CF} + w_O)}\right) \quad (6)$$

$$\theta_{CFB} = \text{acos}\left(\frac{-(d_{VF} + w_O)^2 + w_P^2 + {A_{BC}}^2}{2A_{BC}w_P}\right) \quad (7)$$

$$\theta_{CFE} = \pi - (\theta_{CFA} + \theta_{CFB}) \quad (8)$$

To verify these calculations we conducted a number of sliding and rolling manipulations while recording joint angles and object position. This allowed comparison between predicted object sliding distance Δd_{VF} and pushing finger motion necessary for 90 deg rolling $\Delta\theta_{VF}$. Table 1 shows that the models perform well. We hypothesize that the errors stem from object slip on the high-friction surface and occasional pivoting on the CF finger. These derivations may now be used to plan efficient motions such as sliding an object to an optimal location prior to rolling, given the object size.

VI. Conclusion And Future Work

This work introduces the concept of a biologically inspired variable friction finger pad design that uses a simple passive mechanism to enable within-hand pose manipulation of objects. To demonstrate the practicality of this approach we implemented the design on a simple low-dexterity 2DOF gripper. An unsophisticated controller alternates between

Table 1: Comparing object sliding magnitude (top) and finger angle for rolling (bottom) between geometric models and experimental data

Trial	w_O	d_{CF}	θ_{CF}	$\Delta\theta_{CF}$	Δd_{VF}	$\widehat{\Delta d}_{VF}$	Err (mm)
1	25.4	62	39.3	60.5	50.4	52.7	-2.3
2	25.4	36	38	65.3	51.4	52.41	-1.01
3	38.1	55	55	38	35	36.38	-1.38
4	38.1	34.5	37.5	57.4	50	51.54	-1.54

Trial	w_O	d_{CF}	θ_{CF}	$\Delta\theta_{CF}$	$\widehat{\Delta\theta}_{CF}$	Err (deg)
1	25.4	40	45.3	41.1	42.03	-0.93
2	25.4	52	43.4	42.8	40.34	2.46
3	38.1	29	55.6	64	63.66	0.34
4	38.1	43	48.9	63	66.58	-3.58

torque and position control for each finger, in order to maintain object grasp while also modulating grip force. This

in turn varies finger surface friction to allow sliding, gripping and rolling of objects. The later addition of active fingers (which are able to switch between VF and CF modes) permits controlled sliding of object on both fingers. This extends the capability of the hand and enables such as abilities as in-place rotation or proximal/distal transfer, for the fine positioning of objects within the gripper workspace.

In future work we plan to implement a closed loop controller to achieve target object poses. In particular we plan to integrate vision sensors to eliminate modelling errors due to slip while also investigating machine learning approaches for deriving efficient manipulation strategies. Expanding the manipulation approaches to deal with a wider variety of objects, including asymmetric and compliant objects, is also a potential avenue of investigation. Other goals involve applying the VF framework to higher-DOF (multiple phalanx) and underactuated manipulators (such as the M2 and Model-O OpenHand grippers [22], [34]). This will enable the potential of WIHM to be investigated for more stable grasping techniques while potentially expanding the range of finger motions. Of course, such implementations will increase the complexity of the system and are likely to require to more sophisticated control approaches.

We believe that the relative simplicity of fabricating and controlling the current VF fingers makes this framework applicable to a range of robotic research platforms and topics. In particular, the VF mechanism may be easily integrated into various finger shapes and sizes for a variety of environments and tasks. Indeed, the associated design files will be made open source in time for publication of this manuscript.

REFERENCES

[1] I. M. Bullock and A. M. Dollar, "Classifying human manipulation behavior," in *IEEE International Conference on Rehabilitation Robotics*, 2011.

[2] P. Akella and M. Cutkosky, "Manipulating with Soft Fingers: Modeling Contacts and Dynamics," *Mech. Eng.*, pp. 764–769, 1989.

[3] D. C. Chang and M. R. Cutkosky, "Rolling with deformable fingertips," *Proc. 1995 IEEE/RSJ Int. Conf. Intell. Robot. Syst. Hum. Robot Interact. Coop. Robot.*, pp. 194–199, 1995.

[4] C. Chorley, C. Melhuish, T. Pipe, J. Rossiter, and G. Whiteley, "A Biologically Inspired Fingertip Design for Compliance and Strength," in *Proc. of Towards Autonomous Robotic Systems,* 2008.

[5] M. J. Adams, S. A. Johnson, P. Lefevre, V. Levesque, V. Hayward, T. Andre, and J.-L. Thonnard, "Finger pad friction and its role in grip and touch," *J. R. Soc. Interface*, vol. 10, no. 80, pp. 20120467–20120467, 2012.

[6] C. Chorley, C. Melhuish, T. Pipe, and J. Rossiter, "Development of a Tactile Sensor Based on Biologically Inspired Edge Encoding," *Design*, pp. 1–6, 2009.

[7] M. Cutkosky, J. Jourdain, and P. Wright, "Skin materials for robotic fingers," *Proceedings. 1987 IEEE Int. Conf. Robot. Autom.*, vol. 4, pp. 1649–1654, 1987.

[8] N. Xydas and I. Kao, "Modeling of Contact Mechanics and Friction Limit Surfaces for Soft Fingers in Robotics, with Experimental Results," *Int. J. Rob. Res.*, vol. 18, no. 9, pp. 941–950, 1999.

[9] I. M. Bullock and A. M. Dollar, "A two-fingered underactuated anthropomorphic manipulator based on human precision manipulation motions," *Proc. - IEEE Int. Conf. Robot. Autom.*, vol. 2016–June, pp. 384–391, 2016.

[10] S. E. Tomlinson, R. Lewis, and M. J. Carre, "Review of the frictional properties of finger-object contact when gripping," *Proc. Inst. Mech. Eng. Part J J. Eng. Tribol.*, vol. 221, no. 8, pp. 841–850, 2007.

[11] S. Comaish and E. Bottoms, "The Skin and Friction: Deviations From Amonton'S Laws, and the Effects of Hydration and Lubrication," *Br. J. Dermatol.*, vol. 84, no. 1, pp. 37–43, 1971.

[12] S. E. Tomlinson, R. Lewis, and C. M. J., "The effect of normal force and roughness on friction in human finger contact," *Wear*, vol. 267, no. 5–8, pp. 1311–1318, 2009.

[13] I. M. Bullock, C. Guertler, and A. M. Dollar, "Patterned compliance in robotic finger pads for versatile surface usage in dexterous manipulation," *Proc. - IEEE Int. Conf. Robot. Autom.*, vol. 2015–June, no. June, pp. 2574–2579, 2015.

[14] N. Chavan Dafle, M. T. Mason, H. Staab, G. F. Rossano, and A. Rodriguez, "A Two-Phase Gripper to Reorient and Grasp," in *IEEE Conference on Automation Science and Engineering (CASE)*, 2015,

[15] N. Function, S. Laborat, R. World, and C. Partnership, "Motion Planning for Intelligent Manipulations by Sliding and Rotating Operations with Parallel Two-Fingered Grippers," pp. 119–126.

[16] J. Dejeu, M. Bechelany, P. Rougeot, L. Philippe, "Adhesion control for Micro- and Nano-Manipulation . 2011.

[17] H. Abdi, M. Asgari, and S. Nahavandi, "Active surface shaping for artificial skins," *Conf. Proc. - IEEE Int. Conf. Syst. Man Cybern.*, pp. 2910–2915, 2011.

[18] T. Umedachi, V. Vikas, and B. A. Trimmer, "Highly deformable 3-D printed soft robot generating inching and crawling locomotions with variable friction legs," *IEEE Int. Conf. Intell. Robot. Syst.*, pp. 4590–4595, 2013.

[19] Q. Wu, T. G. Diaz Jimenez, J. Qu, C. Zhao, and X. Liu, "Regulating surface traction of a soft robot through electrostatic adhesion control," *IEEE Int. Conf. Intell. Robot. Syst.*, vol. 2017 pp. 488–493,

[20] L. Winfield, J. Glassmire, J. E. Colgate, and M. Peshkin, "T-PaD: Tactile pattern display through variable friction reduction," in *Proceedings - World Haptics 2007*, 2007, pp. 421–426.

[21] V. Tincani and M. Catalano, "Velvet fingers: a dexterous gripper with active surfaces," *IEEE Int. Conf. Intell. Robot. Syst.*, pp. 1257–1263, 2012.

[22] R. R. Ma and A. M. Dollar, "Yale OpenHand Project: Optimizing Open-Source Hand Designs for Ease of Fabrication and Adoption," *IEEE Robot. Autom. Mag.*, no. March, 2017.

[23] J. Ueda, M. Kondo, and T. Ogasawara, "The multifingered NAIST hand system for robot in-hand manipulation," *Mech. Mach. Theory*, vol. 45, no. 2, pp. 224–238, 2010.

[24] L. Biagiotti, F. Lotti, C. Melchiorri, and G. Vassura, "How Far Is the Human Hand ? A Review on Anthropomorphic Robotic End-effectors Basic concepts," *Hand*, p. 21, 2004.

[25] N. Y. Chong, "A Generalized Motion/Force Planning Strategy for Multifingered Hands using both Rolling and Sliding Contacts," vol. 0, no. C, pp. 113–120, 1993.

[26] F. E. Vina B., Y. Karayiannidis, K. Pauwels, C. Smith, and D. Kragic, "In-hand manipulation using gravity and controlled slip," in *IEEE Int. Conf. Intell. Robot. Syst.*, 2015, vol. 2015–Decem.

[27] J. Shi, J. Z. Woodruff, P. B. Umbanhowar, and K. M. Lynch, "Dynamic In-Hand Sliding Manipulation," *IEEE Trans. Robot.*, pp. 1–18, 2017.

[28] D. L. Brock, "Enhancing the dexterity of a robot hand using controlled slip," *Proceedings. 1988 IEEE Int. Conf. Robot. Autom.*, no. 7, pp. 249–251, 1988.

[29] A. A. Cole, P. Hsu, and S. S. Sastry, "Dynamic Control of Sliding by Robot Hands for Regrasping," *IEEE Trans. Robot. Autom.*, vol. 8, no. 1, pp. 42–52, 1992.

[30] X. Z. Zheng, R. Nakashima, and T. Yoshikawa, "On dynamic control of finger sliding and object motion in manipulation with multifingered hands," *IEEE Trans. Robot. Autom.*, vol. 16, no. 5, pp. 469–481, 2000.

[31] T. Yoshikawa, Y. Yokokohji, and A. Nagayama, "Object handling by three-fingered hands using slip motion," in *International Conference on Intelligent Robots and Systems*, 1993, pp. 99–105.

[32] R. D. Howe and M. R. Cutkosky, "Practical Force-Motion Models for Sliding Manipulation," *Int. J. Rob. Res.*, vol. 15, no. 6, pp. 557–572, Dec. 1996.

[33] S. Goyal and A. Ruina, "Planar Sliding with Dry Friction Part 1. Limit Surface and Moment Function," *Wear*, vol. 143, pp. 307–330, 1991.

[34] R. R. Ma, A. Spiers, and A. M. Dollar, "M2 gripper: Extending the dexterity of a simple, Underactuated gripper," *Mech. Mach. Sci.*, vol. 36, pp. 795–805, 2016.